IL NUOVO CIMENTO **47 C** (2024) 302
DOI 10.1393/ncc/i2024-24302-x

Communications: SIF Congress 2023

Production of antiprotons in cosmic rays with new cross-sections

F. D'Angelo(1)(2)(*), A. Oliva(1) and N. Masi(1)

(1) *INFN, Sezione di Bologna - Bologna, Italy*
(2) *Dipartimento di Fisica e Astronomia, Università di Bologna - Bologna, Italy*

received 30 January 2024

Summary. — Galactic cosmic ray antiproton flux is used to study possible traces of dark matter annihilation. In this work, the background of antiprotons produced by galactic cosmic rays interacting with the interstellar medium has been re-evaluated on the basis of an improved model of antiproton production cross-section and using state-of-art galactic and heliospheric cosmic ray transport codes. We found that the antiproton flux measured by AMS-02 is underestimated by the model of about 3% in the range between 4 and 40 GeV with a significance higher than 6σ, considering only the cross-section uncertainties. However, the full evaluation of the significance of the observed discrepancy depends on other modelization uncertainties, to be estimated in further work.

1. – Introduction

Galactic Cosmic Rays (GCRs) are high-energy particles coming from outer space and are composed mainly of electrons, protons, and completely ionized nuclei. Traces of anti-matter, such as antiprotons and positrons, are present in GCRs and are believed to have mostly originated from the collision of GCR matter with the interstellar medium, composed mostly of Hydrogen and Helium.

The transport of Cosmic Rays in the Galaxy is usually described by a series of coupled diffusion equations that are tuned to reproduce both the GCR primaries, species that have a non-null source term (such as p, He, C, O, Fe), and GCR secondaries, that are produced by primaries collision with ISM (such as Li, Be, and B). The inclusion in the model of antiproton production cross-section measured on the ground on particle beams allows us to predict the antiproton secondary flux.

The antiproton secondary flux, also known as the antiproton astrophysical background, has been carefully compared with the high-precision direct antiproton measurements of AMS-02 [1], looking for possible traces of Dark Matter annihilations that may be evident over the small predicted secondary flux. Some works have found an excess of antiprotons in AMS data between 1 and 100 GeV [2-4], however, other authors insist that such excess is not statistically significant [5-7].

In this paper, an analytical model to estimate the antiproton production cross-section [8,9] has been updated using recent accelerator data. New datasets were released

(*) E-mail: `francesco.dangelo13@unibo.it`

a few years ago [10,11] and experimental efforts are ongoing to improve the cross-section knowledge [12]. The updated production cross-section model has been used to calculate the antiprotons astrophysical background model using the state-of-the-art galactic cosmic ray transport code GALPROP-v.57 [13]. The fluxes from GALPROP have been also corrected for the effect of the transport in the heliosphere by using the HelMod-4 code [14]. This complex multi-parameter model has been extensively tested over all the available precision measurements of CGRs from AMS-02 [15]. The antiprotons have been excluded from the transport model tuning.

2. – Methods

Triple-differential invariant antiproton proton production cross-section has been commonly measured and studied as a function of three phase-space variables such as $\{\sqrt{s}, y, p_T\}$ where $\sqrt{s}$ is the energy in the center of mass reference frame, y is the rapidity, and p_T is the component of the momentum transverse to the collision axis. Other parameters that are used in the study of the cross-section are the transverse mass m_T and the the radial scaling x_R. A review of all the useful kinematics to study the process can be found in [16]. The antiproton production invariant cross-section is estimated using the model described by [8, 9], using the following analytical formula:

$$E\frac{\mathrm{d}^3\sigma}{\mathrm{d}p^3} = C_1 R\sigma_{in}(1-x_R)^{C_2}[1+X(m_T-m_P)]^{-\frac{1}{XC_3}}. \tag{1}$$

The X term in eq. (1) accounts for the high energy behavior of the cross-section and is defined as

$$X = C_4 \log\left(\frac{\sqrt{s}}{\sqrt{s}_{threshold}}\right), \tag{2}$$

where $\sqrt{s}_{threshold} = 4m_p$. The scaling factor R in eq. (1) takes into account the low energy ($\sqrt{s} < 10GeV$) behavior. The R and the p-p inelastic cross-section σ_{in} used in the model have been parametrized according to [9, 17]. Additionally, the contribution of antineutrons and antihyperons produced in p-p collision decaying in anti-proton is included with an additional multiplicative term,

$$\left(E\frac{\mathrm{d}^3\sigma}{\mathrm{d}p^3}\right)_{\bar{p},total} = \left(E\frac{\mathrm{d}^3\sigma}{\mathrm{d}p^3}\right)_{\bar{p}}(2+\Delta_{IS}+2\Delta_\Lambda), \tag{3}$$

where the Δ_{IS} factor takes into account the isospin asymmetry in the decay products, between antiprotons and antineutrons, and Δ_Λ is related to the fraction of antihyperons produced. The energy behaviors of Δ_{IS} and Δ_Λ are parametrized according to [9].

The A-A channels (p-He, He-He, ...) contribution is estimated employing a scaling factor on the p-p cross-section [8, 17],

$$\left(E\frac{\mathrm{d}^3\sigma}{\mathrm{d}p^3}\right)_{A_P+A_T\to\bar{p}} = f_{A_PA_T}\left(E\frac{\mathrm{d}^3\sigma}{\mathrm{d}p^3}\right)_{p+p\to\bar{p}}, \tag{4}$$

where the scaling factor $f_{A_PA_T}$ is given by

$$f_{A_PA_T} = A_p^{C_7}A_{tar}^{C_7}\left[A_P^{C_8}\left(1+\frac{N_P}{A_P}\Delta_{IS}\right)F_P(X_f) + A_T^{C_8}\left(1+\frac{N_T}{A_T}\Delta_{IS}\right)F_T(X_f)\right], \tag{5}$$

where P and T indices label the projectile and the target, N and A are the number of neutrons and total nucleons of the element and F are the fragmentation functions given in [18].

Globally, the model has eight free parameters labeled C_1 to C_8. C_1, C_2, C_3, and C_4 are sensitive to data on p-p collisions, while C_7, and C_8 are more sensitive to heavier channels. The low energy scaling parameters C_5, and C_6 have been taken from [17]. The NA61/SHINE, NA49, STAR, ALICE and CMS experiments have been used in the fitting procedure [10, 19-22], as p-p collisions dataset. These data span a huge energy range from $\sqrt{s} = 7.7\,\text{GeV}$ to $\sqrt{s} = 2760\,\text{GeV}$. Accounting for heavier channels, the p-C collisions data from NA49 experiment [23], and p-He collisions data from the LHCb experiment [11] have been included.

Considering $N^{dataset}$ experimental dataset, each one with N_i^{meas} measurement points, the χ^2 has been defined as [24]

$$\chi^2 = \sum_{i=1}^{N^{dataset}} \sum_{j=1}^{N_i^{meas}} \left(\frac{\Phi_{ij}^{model} - \omega_i \Phi_{ij}^{meas}}{\omega_i \sigma_{ij}^{meas}} \right)^2 + \sum_{i=1}^{N^{dataset}} \left(\frac{\omega_i - 1}{\sigma_i^{scale}} \right)^2, \tag{6}$$

where for each data point Φ^{meas} is the measured cross-section and Φ^{model} is the cross-section calculated with the model for the same point in the three phase-space variables of the measurement. The ω parameter is used as a global normalization factor applied to each dataset. It has been assumed to be Gaussian with unitary mean value and standard deviation σ^{scale}. For each dataset the normalization uncertainty σ^{scale} has been taken from the experimental publication [10, 11, 19-23]. When not available, similar assumptions of [17] have been employed.

3. – Results and discussion

The fit parameters are the following:

$$C_1 = (5.27 \pm 0.012) \times 10^{-2}, \qquad C_5 = 0.000474 \text{ taken from [17]},$$
$$C_2 = 7.918 \pm 0.071, \qquad C_6 = 3.70 \text{ taken from [17]},$$
$$C_3 = (1.668 \pm 0.012) \times 10^{-1}, \qquad C_7 = (8.38 \pm 0.13) \times 10^{-1},$$
$$C_4 = (3.93 \pm 0.10) \times 10^{-2}, \qquad C_8 = (1.12 \pm 0.13) \times 10^{-1}.$$

A total $\chi^2 = 1.5109$ has been obtained considering 757 total degrees of freedom.

The results are consistent with [17]. This production cross-section model has been implemented in GALPROP-v57 and used to calculate the antiproton local interstellar spectrum. The spectrum at Earth's orbit has been calculated employing the latest HelMod code [13-15].

In fig. 1 the comparison with AMS-02 data [1] is shown, together with the prediction using the cross-section models presented in [17]. The predicted flux underestimates the AMS-02 data between 4 and 40 GeV, with a significance of more than 6σ. The inclusion of additional model uncertainties on galactic propagation and solar modulation will decrease sizeably the significance [7, 12]. This is left for a future estimation.

In conclusion, the recent NA61 [10] and LHCb datasets [11] have been included in the modelization of the antiproton production cross-section. This allowed to reduce

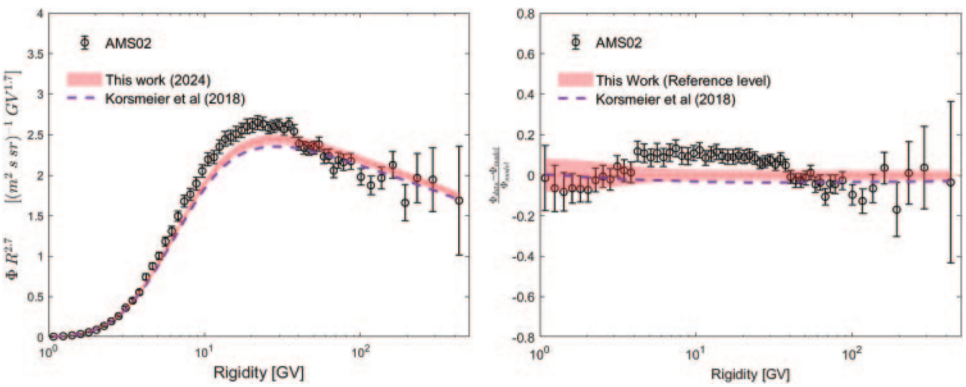

Fig. 1. – On the left, AMS-02 CRs antiproton data are shown, together with the theoretical model presented in this work, *i.e.*, the red 1σ nuclear uncertainty band and the flux prediction (dash-dotted line) within, and ref. [17] analytical prediction (violet dashed line). On the right, the associated residuals, using the present calculation as reference.

the cosmic rays antiproton flux uncertainties due to the production cross-section from 12–15% to 3% in the 10–500 GV range (fig. 1).

* * *

We acknowledge INFN and ASI under ASI-INFN Agreements No. 2021-43-HH.0.

REFERENCES

[1] The AMS Collaboration, *Phys. Rep.*, **894** (2021) 1.
[2] Cholis I. *et al.*, *Phys. Rev. D*, **99** (2019) 103026.
[3] Cuoco A. *et al.*, *Phys. Rev. D*, **99** (2019) 103014.
[4] Lin S. J. *et al.*, *Phys. Rev. D*, **100** (2019) 103014.
[5] Heisig J. *et al.*, *Phys. Rev. Res.*, **2** (2020) 043017.
[6] Di Mauro M. and Winkler W. M., *Phys. Rev. D*, **103** (2021) 123005.
[7] Boudaud M. *et al.*, *Phys. Rev. D*, **99** (2019) 123028.
[8] Winkler M. W., *J. Cosmol. Astropart. Phys.*, **02** (2017) 048.
[9] Kappl R. and Winkler M. W., *J. Cosmol. Astropart. Phys.*, **09** (2014) 051.
[10] The NA61/SHINE Collaboration, *Eur. Phys. J. C*, **77** (2017) 671.
[11] The LHCb Collaboration, *Phys. Rev. Lett.*, **121** (2018) 222001.
[12] The AMBER/COMPASS++ Collaboration, CERN-SPSC-2019-022 (2019).
[13] Moskalenko I. V. and Strong A. W., *Astrophys. J.*, **509** (1998) 212.
[14] Della Torre S. *et al.*, *Adv. Space Res.*, **49** (2012) 1587.
[15] Boschini M. J. *et al.*, *Astrophys. J. Suppl. Ser.*, **250** (2020) 27.
[16] Di Mauro M. *et al.*, *Phys. Rev. D*, **90** (2014) 085017.
[17] Korsmeier M. *et al.*, *Phys. Rev. D*, **97** (2018) 103019.
[18] The NA49 Collaboration, *Eur. Phys. J. C*, **73** (2013) 2364.
[19] The NA49 Collaboration, *Eur. Phys. J. C*, **65** (2010) 9.
[20] The STAR Collaboration, *Phys. Lett. B*, **616** (2005) 8.
[21] The ALICE Collaboration, *Eur. Phys. J. C*, **71** (2011) 1655.
[22] The CMS Collaboration, *Eur. Phys. J. C*, **72** (2012) 2164.
[23] The NA49 Collaboration, *Eur. Phys. J. C*, **73** (2013) 2364.
[24] D'Agostini G., *Nucl. Instrum. Methods Phys. Res. A*, **346** (1994) 306.